Genomic analyses capture the human-induced demographic collapse and recovery in a wide-ranging cervid

Camille Kessler[1], Aaron B.A. Shafer[1,2]

[1]Environmental and Life Sciences Graduate Program, Trent University, Peterborough, Ontario, Canada

[2]Department of Forensic Science, Trent University, Peterborough, Ontario, Canada

Correspondence: camillekessler@trentu.ca (CK), aaronshafer@trentu.ca (ABAS)

Abstract

The glacial cycles of the Quaternary heavily impacted species through successions of population contractions and expansions. Similarly, populations have been intensely shaped by human pressures such as unregulated hunting and land use changes. White-tailed and mule deer survived in different refugia through the Last Glacial Maximum, and their populations were severely reduced after the European colonisation. Here, we analysed 73 re-sequenced deer genomes from across their North American range to understand the consequences of climatic and anthropogenic pressures on deer demographic and adaptive history. We found a strong signal of glacial-induced vicariance and demographic decline; notably, there is a severe decline in white-tailed deer effective population size (N_e) at the end of the Last Glacial Maximum. We found robust evidence for colonial overharvest in the form of a recent and dramatic drop in N_e in all analysed populations. Historical census size and restocking data show a clear parallel to historical N_e estimates, and temporal N_e/N_c ratio shows patterns of conservation concern for mule deer. Signatures of selection highlight genes related to temperature, including a cold receptor previously highlighted in woolly mammoth. We also detected immune-genes that we surmise reflect the changing land-use patterns in North America. Our study provides a detailed picture of anthropogenic and climatic-induced decline in deer diversity, and clues to understanding the conservation concerns of mule deer and the successful demographic recovery of white-tailed deer.

Keywords: Odocoileus, last glacial maximum, island population, human impact

Introduction

The glacial cycles of the Quaternary with movement of ice sheets, corresponding sea level fluctuations, and global environmental changes, heavily impacted worldwide biota (Batchelor et al. 2019; Allen et al. 2020; Gowan et al. 2021). In the northern hemisphere, species adapted to the temperate climate were forced to adapt in cold periods, move or retreat to refugia, their population decreasing or going extinct in the process; warming episodes allowed for population expansion, colonisations, and adaptive divergence (Pamilo and Savolainen 2004; Lorenzen et al. 2011; Martchenko and Shafer 2023). The peopling of North America ~15,000 years ago (kya; Willerslev and Meltzer 2021) followed by human expansion was also a driver of regional ecological shifts (Gajewski et al. 2019; Fulton and Yansa 2021; Commerford et al. 2022), although there is no consensus on whether this was responsible for large mammal declines (Stuart 2015; Meltzer 2020; Stewart et al. 2021).

The more recent Anthropocene has dramatically shaped demographic trajectories of wildlife through farming, hunting and logging (Ceballos et al. 2015; IPCC 2022). Human pressures increased during colonial eras when settlers profoundly altered the land, leading to declines in endemic populations (Woinarski et al. 2015; Lindo et al. 2016; Tavares et al. 2019; Brain and Prosser 2022; Stevens et al. 2022). Indeed, colonial impact has been associated with the extinction of several species such as Australian rodents, and the blue antelope (*Hippotragus leucophaeus;* Roycroft et al. 2021; Hempel et al. 2022). Beyond the demographic impacts, settler populations might also have altered selection pressures, with recent examples of selective harvest including brown bears (*Ursus arctos*) and moose (*Alces alces*; Allendorf and Hard 2009; Kvalnes et al. 2016; Van De Walle et al. 2018).

Severe population contractions, or bottlenecks, increase genetic drift and inbreeding risk, and while highly deleterious mutations can be purged, mildly deleterious mutations tend to accumulate (Frankham 2005; Charlesworth 2009), as seen in alpine ibex (*Capra ibex*) and

woolly mammoth (*Mammuthus primigenius*; Palkopoulou et al. 2015; Grossen et al. 2020). Population size fluctuations also leave discernible genome-wide patterns: a declining population will exhibit a positive Tajima's D and a relatively flat site frequency spectrum (SFS), whereas an expanding population will present a negative Tajima's D and a SFS skewed towards low-frequency or rare alleles (Hahn 2018). Depending on the extent of the contraction, both in magnitude and duration, populations might also present with a low effective population size (N_e), particularly if the bottleneck was strong and the recovery long (Martchenko and Shafer 2023). In contrast, a population that remained steady over time, or one that recovered quickly from a bottleneck, will usually exhibit a larger N_e (Charlesworth 2009). Genomic data can be used to model changes in historical and, due to recent analytical advances, contemporary trends of N_e (Li and Durbin 2011; Schiffels and Durbin 2014; Santiago et al. 2020; Schiffels and Wang 2020), and when compared to census size (N_c), both historical and contemporary estimates of N_e/N_c reflect adaptive potential and extinction risk (Palstra and Ruzzante 2008; Wilder et al. 2023).

The species of the North American genus *Odocoileus* (deer) were heavily impacted by the glacial cycles of the Pleistocene and European colonisation. Divergence estimates suggest the speciation between white-tailed (*O. virginianus*; WTD) and mule deer (*O. hemionus*; MD) took place between 500 kya and 4.3 million years (Mya; Baccus et al. 1983; Kessler et al. 2023), the genus became among the most successful Cervids during glacial cycles (Hewitt 2011). Both species survived in different refugia during the Last Glacial Maximum (LGM, 26 - 19 kya (Clark et al. 2009); Ellsworth et al. 1994; Greenslade 1998; Latch et al. 2009; Latch et al. 2014) and share mitochondrial haplotypes due to incomplete lineage sorting (Klicka et al. 2023). While WTD & MD hybridise (eg. Carr and Hughes 1993; Russell et al. 2021), the hybridisation appears to be a result of secondary contact and did not impact speciation (Kessler et al. 2023).

Deer abundance is heavily monetised through hunting-related activities in North America (Cambronne 2013), and both species have been, and continue to be, important to indigenous communities as a source of food, clothing and culture (Adams and Hamilton 2011; Peres and Altman 2018). In the late Holocene, WTD were likely the most abundant large-mammal prey in eastern North America, and while some Indigenous Peoples depended on them for subsistence, harvest appeared to minimally impact WTD numbers (Wolverton et al. 2008; Weitzel 2021). In contrast, over-hunting and forestry practices post European-colonisation resulted in heavily depleted and even extirpated WTD populations, leading to strict hunting regulations followed by restocking efforts across the USA in the 20th century (McDonald et al. 2004), with stocking efforts leaving discernible admixture patterns in WTD genome (Chafin et al. 2021). Mule deer abundance is, and was, lower than WTD; their populations also declined post-colonisation and plunged in the early 1900's (Jensen et al. 2023). Stocking efforts were less pervasive for MD, and the species stabilised due to effective management strategies (Gruell 1986; Clements and Young 1997; Gill 1999; Bergman et al. 2015; Jensen et al. 2023). Previous historical demographic analysis for both species have generated both contrasting and coarse demographic reconstructions (Combe et al. 2021; Lamb et al. 2021).

Here, we aim to understand the consequences of climatic and anthropogenic pressures on WTD & MD populations through explicit demographic modelling and selection analyses. We hypothesise that the population genetic histories of North American deer were heavily impacted by the glacial cycles of the Pleistocene and by European colonisation, not the initial peopling of North America. Specifically, we predict that the LGM had a strong negative impact in the form of demographic contraction and population subdivision, and that the impact of European colonisation, notably overhunting and change in land use, would leave detectable signatures on the genome in a neutral and adaptive context. To test these predictions, we used whole genome sequence data of MD and WTD from across their North American range to

compute summary statistics, reconstruct and model demographic histories, and quantify genomic variation linked to environmental factors and selective forces.

Materials and Methods

Sampling & Sequencing

We sequenced the genomes of 45 deer collected across North America (Fig. 1A, Table S1) and added WGS data from 28 published deer genomes (PRJNA830519; Kessler et al., 2023). The complete dataset comprised 20 MD and 53 WTD samples, including four WTD individuals from the Florida Keys subspecies (*O. v. clavium*). We extracted DNA using the Qiagen DNeasy Blood and Tissue Kit following manufacturer's instructions and checked concentration using Invitrogen Qubit assays. DNA was sent to The Centre for Applied Genomics in Toronto, Canada, for library preparation following the Illumina TruSeq PCR-free DNA Library Prep, and sequencing to generate 150bp paired end reads. All samples were sequenced to an average of 4x coverage on an Illumina HiSeqX, except for four samples which were re-sequenced to achieve higher coverage (>15x; Table S1, Fig. 1A). This 4x coverage was targeted as we generated genotype likelihoods that are designed for lower coverage data (Meisner and Albrechtsen 2018).

We obtained estimated census data for WTD and MD in the USA for the last 400 years from Webb (2018; complemented by Deer Friendly). This census data was generated using a process of environmental scanning that aggregated data from different sources such as state agencies, harvest records and historical sources for the most ancient timepoints. We also digitised restocking information for WTD in the USA from McDonald et al. (2004).

Data processing

We analysed and trimmed raw reads with FastQC (v0.11.9; Andrews 2010) and Trimmomatic (v0.36; Bolger et al. 2014), respectively. Using bwa-mem and default settings (v0.7.17; Li and Durbin 2009), we aligned raw reads to the WTD genome (GCA_014726795.1)

and sorted the reads using SAMtools sort (v1.10; Li et al. 2009). We identified and removed duplicates in Picard MarkDuplicates (v2.23.2; Broad Institute, GitHub Repository. 2019) and Sambamba view (v0.7.0; Tarasov et al. 2015). We used GATK RealignerTargetCreator and IndelRealigner (v4.1.7.0; McKenna et al. 2010) to carry out a local re-alignment and used Sambamba flagstat, mosdepth (v0.3.1; Pedersen and Quinlan 2018) and MultiQC (v1.10; Ewels et al. 2016) for quality checks.

For samples sequenced on multiple lanes, we specified the read groups before removing duplicates and merged the sequencing files using Picard AddOrReplaceReadGroups and MergeSamFiles, respectively. To have a consistent coverage among samples for non-SMC demographic analyses, we down-sampled data to the average coverage of all other samples (4x) using Picard DownsampleSam. We called the genotypes (-doGeno 4) and estimated genotype likelihood using the GATK model (-gl 2) in ANGSD (v0.918; Korneliussen et al. 2014). We retained SNPs with a minimum base quality and a minimum mapQ quality of 20 (-minQ 20 & minMapQ 20) and a minimum p-value of 1e-6 (-SNP_pval 1e-6).

Population subdivisions and summary statistics

We used PCAngsd (v1.02; Meisner and Albrechtsen 2018) to investigate population clustering between and within species, this program fits best our data as it is designed explicitly for low-coverage data and genotype likelihoods. We explored the relationship between the spread on the PCA and the geographic distribution of our samples using a Pearson's correlation test in R (v4.2.0; R Core Team 2021). We further generated an individual genetic distance matrix using the gene.dist() function from the ape R package (Paradis and Schliep 2019), with the dataset produced for the δaδi analysis (see below). Finally, to help decipher population structure in the MD samples, we further ran NGSadmix (Skotte et al. 2013), using K = 1 : 10 and 10 replicates, we identified the best K value using CLUMPAK (Evanno et al. 2005; Kopelman et al. 2015). We introduce the following convention to refer to populations

supported by PCAngsd and NGSadmix and used in subsequent analyses: mainland WTD = WTD_{ML}, Florida Keys WTD = WTD_{KEY}, MD subspecies = MD_{MD}, and MD black-tailed deer subspecies = MD_{BTD}.

We computed the genome-wide Tajima's D for all populations following the ANGSD pipeline (http://popgen.dk/angsd/index.php/Thetas,Tajima,Neutrality_tests). Briefly, we produced a folded SFS with angsd -doSaf 1 and realSFS, computed theta with realSFS saf2theta followed by Tajima's D using thetaStat. Further, we converted the hardcalls generated in ANGSD (.geno file) into a .vcf file using a python script (genoToVCF.py; Martin 2021) and retained only biallelic sites (--max-alleles 2) in VCFtools (v0.1.16; Danecek et al. 2011). Using VCFtools we computed weighted F_{st} between the four populations, and nucleotide diversity (π) per population, all processed in windows of 50kbp. We used PLINK (v1.90b6.21; Chang et al. 2015) to estimate the inbreeding coefficient based on runs of homozygosity (F_{ROH}) on the 160 scaffolds representing the N90 of the WTD's genome assembly, using the following non-default criteria: 100kb window size containing a minimum of 50 SNPs, allowing up to three heterozygote sites and 10 missing calls per called ROH. We computed F_{ROH} per individual using the sum of ROH sizes divided by the sum of N90 scaffolds length.

Historical and recent demographic inference

We inferred the historical demography of WTD_{KEY}, WTD_{ML}, MD_{MD} and MD_{BTD} by implementing the multiple sequentially Markovian coalescent (MSMC) model (Schiffels and Durbin 2014) that generates estimates of N_e over time. Here, we used four high-coverage samples, one per population (Fig. 1A, Table S1), and first generated a 35-mer mappability mask file using SNPable, as required for MSMC with several samples (Schiffels and Wang 2020). Because of the small sample size of high coverage genomes, we phased the data with WhatsHap (v1.3; Patterson et al. 2015; Martin et al. 2016) and filtered out scaffolds shorter

than 500 Kbp. We ran MSMC2, including 100 bootstraps, using 1×2+25×1+1×2+1×3 as time segment pattern. To estimate the cross-coalescence rate (CCR) across populations, we carried out a pairwise comparison of the first haplotype from each sample using the -P flag, skipping any site with ambiguous phasing. Finally, to test and account for ancestral migration, we implemented MSMC-IM (Wang et al. 2020), assuming a generation time of 2 years (Deyoung et al. 2003) and a mutation rate of 1.23×10^{-8} mutations/site/generation (average from Table S16 in Chen et al. 2019). We complemented this inference with a stairway plot analysis (v2.1.2; Liu and Fu 2015; Liu and Fu 2020) to reconstruct historical population size changes. Using each population, we generated a folded site frequency spectra in easySFS (v0.0.1; Gutenkunst et al. 2009) and used the resulting SFS as input to stairway plot, along with the same mutation rate and generation time as used for MSMC2.

We used GONE (Santiago et al. 2020) to compute demographic history in the recent past from patterns of linkage disequilibrium (LD) for the four populations. We restricted this analysis to the 160 scaffolds representing the N90 of the WTD assembly. We ran GONE with 500 repetitions on 500 generations with 30,000 SNPs per chromosome, a minor allele frequency pruning of 0.01, a hc value of 0.04, a recombination rate of 0.5 for WTD populations and 0.35 for the MD populations (Kessler et al. 2023). We compared the census size (N_c) point estimates from Webb (2018) to the temporal estimates of N_e resulting from GONE to obtain a contemporary N_e/N_c ratio over time.

We further filtered the dataset in VCFtools to I) account for LD by removing sites that were within 10kbp of each other (--thin 10000), and II) remove all missing data (--max-missing 1). To model explicitly the demographic history of WTD and MD, we used δaδi (v 2.1.1; Gutenkunst et al. 2009) and dadi_pipeline (v3.1.7; Portik et al. 2017) and performed two different demographic analyses with different outgroups: 1) WTD_{KEY}, WTD_{ML} and all MD, and 2) MD_{MD}, MD_{BTD} and WTD_{ML}. We selected relevant demographic models involving

migration and asynchronous splitting (Table S2), optimised and fitted the models with four repetitions and default settings, the best model was selected based on the log-likelihood and its consistency across runs. This model was additionally run with 100 bootstrapped frequency spectrums to quantify uncertainty. We obtained ancestral N_e/N_c ratio over time for both species using the ancestral N_e (NuA) from the δaδi analyses.

Adaptive divergence and selection scans

We used a redundancy analysis (RDA) to detect genotype-environment association and loci under local adaptation across individuals, RDA is a multivariate regression method that allows to identify loci associated with a variety of predictors (Legendre and Legendre 2012). In our case, the predictors are 19 bioclimatic variables (Table S3) which we collected at a resolution of 2.5' from WorldClim2 using the R package raster (v.3.6-3; Hijmans 2022; Fick and Hijmans 2017) and extracted the values corresponding to our samples' coordinates. We performed three analyses: one inter-specific with all individuals, and two intra-specific for WTD & MD using 19 bioclimatic variables, latitude, longitude, and species as predictors. As highly correlated variables are problematic in RDAs, we removed those that showed a Pearson correlation > 0.7 in each analysis (Dormann et al. 2013). We carried out the RDA with the R package vegan (v.2.6-4; Oksanen et al. 2022) based on the datasets created for demographic modelling. In addition to full models including non-correlated predictors, we investigated conditional models with the condition set as either the bioclimatic variables or longitude.

To detect regions under selection in the four populations, we computed the integrated haplotype score (iHS) on the scaffolds representing the N90 of the WTD reference genome. This statistic is based on extended haplotype decay to detect selective sweeps by comparing the state of decay between ancestral and derived allele (Sabeti et al. 2002; Voight et al. 2006). The state of decay for all alleles should be similar in neutral regions and iHS should equal zero in the absence of selection. In the case of a selective sweep and as one allele will rise in

frequency, haplotype decay will be slower and iHS values will become either positive or negative depending if the sweep takes place on the ancestral or derived allele, respectively (Voight et al. 2006). As this analysis included all samples, we started by phasing our data in SHAPEIT (v2.r904; O'Connell et al. 2014), then calculated and normalised iHS in vcflib (v1.0.3; Garrison et al. 2022) with the functions iHS and normalize-iHS and default settings. We identified peaks in the most extreme 1% iHS values in R using the function findPeaks (Grinberg 2019) and extracted gene IDs within 25Kbp upstream and downstream. The genes with available entry IDs were uploaded to Uniprot (Pundir et al. 2016) for ID mapping where we retrieved the gene names and functions. The gene list was manually curated, and each gene was assigned to one or more of the following categories based on its function: reproduction, immunity, physiology, metabolism, sensory perception, development, and other. We analysed all results and produced all the graphics in R.

Results

Population subdivisions and summary statistics

We called 144,634,190 SNPs across species from 73 individuals at a coverage of 4x on average. The PCA on allele frequencies of all individuals presents a clear species delimitation along PC1 which explained 46% of the variation, whereas PC2 separated the WTD_{KEY} individuals (Fig. 1B). WTD-specific PCA showed the delimitation between WTD_{ML} and WTD_{KEY} individuals (PC1); PC2 strongly correlated with longitude (Pearson correlation = -0.88, p-value = < 2.2e-16) and accounted for 7% of the variation (Fig. S1A). In the MD PCA, PC1 correlated to longitude (Pearson correlation = 0.83, p-value = 5.96e-06), and PC2 associated to latitude (Pearson correlation = 0.47, p-value = 0.037, Fig. S1B). The MD PCA showed one clear cluster of 13 samples; we clarified the population identity of the seven remaining individuals using NGSadmix that assigned two admixed individuals to the first cluster (MD_{MD}) and identified a second population of five individuals (MD_{BTD}; Fig. S1C).

Individual genetic distances separated MD and WTD_{KEY} individuals from WTD (Fig. S1D). The individual genetic distance mirrored nucleotide diversity estimates which were highest in WTD_{ML} and similar in the other three populations (Table 1, Fig. S1D).

Weighted F_{st} measures were high in between species comparisons (0.36 - 0.58); intra-specific comparisons ranged from 0.12 to 0.17 (Table S4). Tajima's D values were negative only for the WTD_{ML} population (-0.76), the highest being 1.08 for MD_{BTD} (Table 1,Fig. S2A). F_{ROH} values were lowest in the MD populations (<= 0.3%), whereas WTD_{KEY} presented the highest F_{ROH} value (1.4%; Table 1; Fig. S2B).

Demographic inferences

We inferred the demography of four high-coverage samples, one per population, using MSMC2. The trajectories of the four samples split at approximately 600 kya where the MD_{MD} population start declining whereas WTD populations keep increasing (Fig. 2A). Both MD population trajectories are very similar and show a general steady decline. WTD_{KEY} appear to decline ~50 kya, whereas WTD_{ML} drastically increased to peak at an N_e of >1 million individuals, followed by a clear crash at the end of the LGM (Fig. 2A). Species split times inferred by the cross-coalescence rate of the MSMC-IM model is approximately 500 kya (Fig. S3A), the within-species split times are estimated at ~ 25 kya between WTD_{ML} and WTD_{KEY}, and ~70 kya for MD_{MD} and MD_{BTD} (Fig. S3B). Effective population size over time as inferred by the stairway plot analysis showed similar historic trajectories where all populations have declines surrounding the LGM (Fig. S4). However, both MD_{BTD} and WTD_{ML} presented a large recovery post-LGM followed by a recent crash; this is consistent with model overfitting in a stairway plot that produces spurious and complex patterns (Lapierre et al. 2017).

The N_e of WTD_{KEY} appears very low and stable for the last ~400 years, reaching its lowest at ~350 individuals (Fig. 2B). Temporally, the WTD_{ML} population decreased with variable intensity that ended with a drastic decline to a N_e of ~2000 near the end of the 19th

century. Following this severe drop, the WTD_{ML} population rapidly rebounded to reach a current effective size in the millions (Fig. 2B); this clearly correlates with census data and restocking efforts (Fig. 2C). Both MD populations exhibited a slow but steady increase until approximately 300 years ago, after which both trajectories show a gradual decline ending with a severe drop without recovery (Fig. 2B). MD N_e patterns are more decoupled from the census data as N_c here shows a crash in both MD_{MD} and MD_{BTD} followed by a small recovery (Fig. 2C). As such, the contemporary N_e/N_c ratio is higher and more variable for MD (Fig. 3; mean = 0.49, var = 0.3 vs WTD mean = 0.18 & var = 0.01) with most values from the last century below 0.1. Both species have a low ancestral N_e/N_c ratio with low variability, the averages are of 0.06 and 0.01 for WTD and MD, respectively. White tailed deer's historical ratio (var = 0.03) is more variable than MD (var = 0.0001) and the contemporary WTD (Fig. 3).

Finally, we modelled the demographic history of our four populations using the site frequency spectra. For our first comparison, we analysed the demographic history of the trio WTD_{KEY} – WTD_{ML} – MD, the best model supports adjacent secondary contact between populations, however migration rates remain low ($m < 1e^{-5}$; Fig. 4A, Table S5). This model suggests a MD/WTD split ~280 kya followed by a MD decline and a WTD expansion. After the split between WTD_{KEY} and WTD_{ML}, both populations declined with notably a demographic crash in WTD_{KEY}; all of these predate the peopling of North America. In our second trio, we investigated the relationship between MD_{MD} – MD_{BTD} – WTD_{ML}. In this case, the split WTD/MD is seen ~390 kya, the best model suggests a secondary contact between WTD_{ML} – MD_{MD} that predates the split between the two MD populations, ~13 kya, but all migration rates are extremely low ($m <= 4e^{-6}$). This model also suggests population expansion for WTD_{ML} after the split from MD, but a decline for both MD_{BTD} and MD_{MD} before and after the peopling of North America (Fig. 4B, Table S5).

Adaptive divergence and selection

We conducted three redundancy analyses to identify genotypes linked to environmental variables and loci under local adaptation. The RDA with all individuals explained 16.5% of the variation, most of which was driven by the species variable (Table 2, Fig. S7A). The full model for the WTD explained 6.32% of the variation and included five significant predictors - BIO1 (annual mean temperature), BIO2 (mean diurnal range), BIO8 (mean temperature of wettest quarter), BIO15 (precipitation seasonality) and longitude (Table 2, Fig. S7B). There were 12,206 outlier SNPs, predominantly associated with annual mean temperature (Table 2 & S3, Fig. S7C). In the RDA on MD, we found only BIO2 and BIO16 (precipitation of wettest quarter) as significant predictors, and 7434 outlier SNPs, mostly associated with BIO16 (Table 2). Conditional models of bioclimatic variable explained more variation than those of longitude in both species (Table 2).

We found a total of 443 genes within 25 Kbp upstream and downstream of an iHS peaks, including 249 with an existing Entry ID (Table S6). There were 121 genes around iHS peaks in the WTD_{ML} population, 45 of which we could assign an explicit category including 18 genes assigned to immunity, of which two related to the major histocompatibility complex (MHC): *HLA-DQA1* and *HLA-DQB*. Additionally, we found two genes linked to sensory perception: one odorant receptor (*OR5D18*) and one cold receptor (*TRPM8*, Table S6). We identified 23 genes surrounding iHS peaks in the WTD_{KEY}, including one MHC gene: *HLA-DRB4*. For the MD_{MD} population, we could explicitly categorise 34 genes on a total of 95 neighbouring iHS peaks. They include four MHC genes: *HLA-DQA1*, *HLA-DQB1*, *HLA-DRB3* and *HLA-DRB4*, another gene related to the MHC: *HIVEP2*, three genes described as olfactory or odorant receptors (*OR51I1*, *OR5D18*, *TAAR5*), and one cold receptor (*GRIK2*). Finally, we identified 26 genes adjacent to iHS peaks in the MD_{BTD} population, including two related to immunity and three linked to reproduction.

Discussion

The complex climatic cycles of the Pleistocene, concluding with the LGM, generally forced species to move from a wide range into smaller, often isolated refugia (Soltis et al. 2006; Shafer et al. 2010). The peopling of North America and the colonisation by Europeans several millennia later represented further pressures to many populations inhabiting the continent (McDonald et al. 2004; Lindo et al. 2016; Smith et al. 2021). Here, we reconstructed the demographic history and signals of selection of WTD & MD to improve our understanding of climatic and anthropogenic pressures on these two North American species. Through extensive genomic analysis we observed a remarkable overlap between climate, recent human drivers, and N_e, and provide a temporal N_e/N_c assessment supporting the demographic concerns facing MD (Bergman et al. 2015; Webb 2018). Further, our selection scans that reflect climate and disease pressures provide testable hypotheses for the impact of European colonisation.

Strong historical climatic impact on deer populations

The glacial cycles of the Quaternary forced populations to move or adapt, resulting in population divergence (Colella et al. 2021; Ito et al. 2021), decline (Ersmark et al. 2019; Baca 2020; Dussex et al. 2020; Meiri et al. 2020) and even replacement (Loog et al. 2020). Our results suggest a clear impact of climate on WTD during the late Quaternary as we observed an intense N_e drop for WTD_{ML} as well as a population split time that coincides with the LGM (Fig. 2A, Fig. S3A), and support WTD populations being separated into different refugia during this period (Ellsworth et al. 1994; Moscarella et al. 2003; Combe et al. 2021; Wright et al. 2022). The Key deer showed a steady decline that predated the LGM, with a clear separation from WTD_{ML} ~50 kya (Fig. 2A, Fig. 4A, Table S5). All analyses suggest both populations started diverging before the isolation of the Florida Keys from the continent ~8,000 years ago (Ellsworth et al. 1994; Villanova et al. 2017). This isolation led to a clear loss of genomic diversity (Table 1, Fig. S2) and accumulation of deleterious alleles in the endangered Key deer

(Cars et al. 2023; U.S. Fish & Wildlife Service 1967). Overall, the collective demographic methods used here pinpoint the LGM as a driver of subdivision and historical declines in WTD.

The LGM has also been implicated in the MD and BTD (*O. h. columbianus*) subdivision, as the two subspecies were separated in different refugia during that time (Latch et al. 2009; Latch et al. 2014; Wright et al. 2022). Our results are equivocal regarding the split time: the MSMC analysis suggest a steady decline of both populations and a MD/BTD split estimated at approximately 70 kya by the CCR (Fig. 2A, S2B); δaδi analysis, in contrast, places the split after the LGM and concomitant with a decline of ~30% in both populations (Fig. 4B, Table S5). While we present here the best model for our data, both comparisons still present with relatively large residuals (Fig. 4) suggesting the true story might be more complicated than depicted here. Additional modelling with different approaches might help render a more precise history. Nevertheless, both analyses support changes pre-peopling of North America and are consistent pre-split: the N_e of the common ancestor of MD_{MD} and MD_{BTD} appeared low but stable through time (Fig. 2A). As MD are more prone to population fluctuations (Forrester and Wittmer 2013), and N_e is most strongly influenced by long periods of low N_c (Peart et al. 2020), the overall stable historical N_e is consistent with population genetic theory.

Hahn (2018) suggested to focus on big picture, not point estimates, for demographic inferences, and while MSMC reconstructions differ in magnitude based on data treatment, overall time and shape remains constant (Schiffels and Wang 2020). While the general historical patterns of demographic change observed here support previous assessments (Lamb et al. 2021), including the LGM impact in WTD, they are in contradiction with Combe et al. (2021). Combe et al's (2021) stairway plot analysis of ~25k SNPs suggests a single population contraction ~100 kya followed by an expansion for WTD, and population plateau at high number for over 200 kya before a drastic decline for MD. These times are inflated due to their generation time of five years versus two used here (see also Deyoung et al. 2003). Simulations,

have shown that a dataset of this size is cannot reliably resolve changes in N_e (Shafer et al. 2015), thus our explicit modelling and genome-wide data set has significantly more power and precision with respect to historical demographic inference. Further stairway plots are prone to over-fitting and erroneous reconstructions (Lapierre et al. 2017). For example, the explosive LGM recovery suggested by our WTD_{ML} stairway plot is at odds with our all other results and patterns seen in comparable species (e.g. Dussex et al. 2020; Taylor et al. 2021).

None of the deer populations analysed here showed any signal of recovery after the LGM and ice sheets recession. This is particularly striking given the massive loss of large mammals on the continent (Elias and Schreve 2007; Stuart 2015; Meltzer 2020), presumably opening new niches, reducing competition and predation. One explanation could be that the primary cause of population declines in deer were the environmental shifts caused by the deglaciation dynamics (Mottl et al. 2021; Hanberry 2023) and the changes in ecosystem function after the megafaunal extinctions (Malhi et al. 2016; Malhi et al. 2022). The lack of full recovery is consistent with population dynamics of other temperate ungulate species (De Jong et al. 2020; Dussex et al. 2020; Taylor et al. 2021; Robin et al. 2022). Nevertheless, the limits of detection of MSMC2 and GONE (10 kya – 0.4 kya) do leave a gap in the Holocene for which it is difficult to reconstruct demographic history; however, δaδi should pick up a large Holocene change (e.g. Dedato et al. 2022), or the pattern seen in the stairway plot analysis, were they to have actually occurred.

Hybridisation between WTD and MD in areas of sympatry is well documented (eg. Cronin 1991; Derr 1991; Carr and Hughes 1993), but it was suggested that introgression had no impact on species divergence and rather that gene flow is a result of secondary contact (Kessler et al. 2023). Likewise, Klicka et al. (2023) suggested incomplete lineage sorting of mitochondria, not historical hybridisation, explains shared haplotypes between species. This is consistent with our analyses as both δaδi comparisons suggest a secondary contact with low

migration rates (Fig. 4, Table S5), and while some ancient migration is detected, it is extremely low (Fig. 4B, Table S5, Fig. S3C). Our results therefore support the finding of negligible ancient gene flow between species. In fact, our analyses suggest a species split time under 500 kya (Fig. 4, Table S5, Fig. S3), which are more recent than previous molecular clock evaluations ranging between 750 kya and 4.3 mya (Baccus et al. 1983; Douzery and Randi 1997; Combe et al. 2021; Wright et al. 2022). All of these estimates were based either on a restricted number of nuclear and mitochondrial loci, presenting lower power of analysis than our whole genome assessment.

Human-induced collapse, varying selection pressures on white-tailed deer

Driven by overharvest and change in land use for agriculture and logging, the recent decline and near extirpation of WTD has been thoroughly documented in the USA (McDonald et al. 2004). The reconstructed demographic trajectory of the mainland WTD population mirror these historical sources and census size estimates (Fig. 2B-C); specifically, we capture the gradual decline followed by dramatic collapse at the end of the 19th century. This depletion led authorities to implement protective laws and managers to supplement deer populations with translocations (see McDonald et al. 2004 for an extensive summary). Those measures were responsible for the quick rebound we observed for the WTD_{ML} population (Fig. 2B) as analyses of nearly extirpated populations suggest the WTD bottleneck had minimal impact on diversity thanks to the rapid population expansion following translocations (Deyoung et al. 2003; Budd et al. 2018). Together with the stable relationship of N_e/N_c over time we observed (Fig. 3), these results suggest that WTD are highly resilient; however, despite the recovery and high diversity, assessment of deleterious alleles also showed a high genetic load for WTD (Cars et al. 2023; Wootton et al. 2023).

Given the low N_e and stocking efforts of WTD, it is probable that any sweep that took place before the demographic collapse was either lost or fixed, with the latter generally having

reduced power in haplotype scans (Szpiech 2021). In contrast to ungulates experiencing reduced human intervention (e.g. Martchenko and Shafer 2023), longitude had a minimal impact in our models which is consistent with stocking efforts largely erasing geographic signals. Combined with evidence showing rapid contemporary evolutionary responses (Zamorano et al. 2023), we suggest that the outliers and sweeps detected in our analyses could be the result of selection during European colonisation that coincided with large changes to the landscape. In mainland WTD, we found a variety of immunity-related genes potentially under selection which would suggest selection pressures from pathogens (Table S6), some of which might have arisen recently from livestock (Campbell and VerCauteren 2011). The presence of selection at immune genes in WTD scans is consistent with the development of agriculture and large land use changes that have transpired in North America over the past two centuries. Nevertheless, as immune genes are often detected in genome scans and as hyper-variable regions of the genome such as the MHC are susceptible to misalignments (Manel et al. 2016), these results should be taken with caution. Recent selection at immune loci, and indeed the colonial impact, could be investigated by using historical samples: here, any sweep signal detected in the present analysis not seen in historical or ancient DNA would suggest a colonial selection event.

We also found selection patterns at the gene *TRPM8* conferring sensitivity to cold temperature (Table S6); mutations identified in woolly mammoth's *TRPM8* were suggested to be linked to the species' adaptation to cold climates (Lynch et al. 2015). Interestingly, in the RDA between species, as well as in the WTD RDA, most outlier SNPs are associated with mean annual temperature (BIO1) rather than species or longitude meaning that temperature is a major driver of differentiation. WTD are exposed to a wide range of temperatures on the continent, but also rapidly expanding northward (Dawe and Boutin 2016). As climate change clearly impacted historical and contemporary WTD ranges (Dawe and Boutin 2016), outliers

and selection on genes like *TRPM8* are expected, and likely partly responsible for the success of WTD on the continent. Only few genes were identified as under selection for MD_{BTD} and WTD_{KEY}, given the fewer number of samples from those populations the power of the selection scans analysis was clearly reduced (Klassmann and Gautier 2022).

Delayed collapse but similar selection pressures on mule deer

Human Settlements on the MD historic range were estimated at less than 20 in 1800, and while harvest likely depressed populations in the surrounding areas, the rest of the range probably saw minimal impact (Jensen et al. 2023). Over time and with the increased settlements in western North America, MD populations strongly declined to reach their lowest at the end of the 19th century (Gill 1999; Bergman et al. 2015; Jensen et al. 2023). This is consistent with our analysis which shows a sharp decrease in the MD_{MD} population during that period, though the MD_{BTD} population decline appeared later (Fig. 2B). These population reductions also appeared to happen after the WTD collapse, possibly reflecting the later western wave of settlers and more recent land use changes. As a migratory species, MD might respond more to human-induced habitat change, for example, the limitation in winter range habitat appears to be driving MD decline in Colorado (Gill 1999; Bergman et al. 2015). Collectively the delayed decline, the decoupling of N_e from N_c (Fig. 3), the positive Tajima's D and the more muted temporal response of N_e are consistent with the species ecology and human intervention history. Despite this collapse and lack of recovery, both MD subspecies exhibit relatively high genetic diversity and low F_{ROH} (Table 1, Fig. S2B), all promising signals for a species that is often described as declining. Assessment of MD genetic load should help further inform the management challenges facing this species.

In MD_{MD}, we found 14 immunity-related genes under selection (Table S6). Diseases affecting MD are often the same that infect WTD, including the risk of spilling over to and from livestock (Campbell and VerCauteren 2011). Chronic wasting disease is of particular

concern for MD as it is considered as a major factor in the species decline in many regions (DeVivo et al. 2017), with the genomic and immune response clearly polygenic (Seabury et al. 2020). Regarding sensory perception, we found selection patterns at the cold receptor *GRIK2*. Cold adaptation might have been a determinant factor for MD as they favour higher elevation habitats (Anthony and Smith 1977; Brunjes et al. 2006), and are more tolerant to cold climates (Mautz et al. 1985). Supporting this was outliers associated with mean diurnal range (BIO2), which is linked to temperature (Table S63). Most outlier SNPs were associated with precipitation of the wettest quarter (BIO16, Table 2), likely reflective of MD_{BTD} inhabitation of temperate rainforests (Heffelfinger and Krausman 2023).

Variable N_e/N_c ratio through time

The N_e/N_c ratio is informative on the genomic health and demographic histories of species, which is why it has often been used to assess populations of management and conservation concern (Frankham 1995; Palstra and Ruzzante 2008; Ferchaud et al. 2016). Indeed, a population exhibiting a low contemporary N_e/N_c ratio is more subject to rapid loss in genetic diversity than populations with a higher ratio (Frankham 1995; Palstra and Ruzzante 2008). While, this ratio is highly variable between taxa, the generally accepted median of concern in wild populations is 0.1 (Frankham 1995; Waples et al. 2013). Our unique integrated approach allowed us to measure this ratio over time, with the seven most recent values for MD all below 0.1 (Fig. 3). The larger fluctuations in MD's N_c in the last 100 years appear to have led to a decoupling of N_e and N_c and reflect the species higher demographic stochasticity. This recent reduced ratio could mean that the species is at risk of faster loss of genetic diversity and echoes other calls of concern (Gill 1999; Bergman et al. 2015). Interestingly, historical N_e/N_c ratio presents low variability for both species and no immediate red flag (Wilder et al. 2023); this ratio is clearly driven by the high N_c of both species, and focused sampling of isolated populations might reveal a different pattern as seen in caribou (Dedato et al. 2022). Denser

sampling of MD might also help identify key corridors facilitating gene flow (e.g. Fusco et al. 2023).

Conclusion

We observed strong signals of climate- and human-induced demographic declines with a remarkable overlap between both census and biogeographic data and historical inferences coming from multiple methods. The dramatic drop in N_e in the recent past of all deer populations studied here is robust evidence for a colonial impact through unregulated hunting and changes in land use. Even though WTD & MD populations were heavily depleted, both species showed signs of recovery, particularly white-tailed deer from restocking efforts. While diversity and demographic trends appear positive, there is also a high genetic load in WTD (Wootton et al. 2023), and a low contemporary N_e/N_c ratio in MD. Selection surrounding a wide variety of genes, including some of biological importance in WTD & MD such as genes related to immunity and temperature appear evident. Historical sampling of *Odocoileus* will prove informative for disentangling human-induced selection and genetic load in these wide-ranging cervids.

Acknowledgements

Camille Kessler was supported by an International Graduate Scholarship, an Ontario Graduate Scholarship, and a French American Charitable Trust Scholarship. This work was supported by NSERC Discovery Grant (Grant Number: RGPIN-2017- 03934); ComputeCanada Resources for Research Groups (Grant Number: RRG gme-665-ab); Canadian Foundation for Innovation: John R. Evans Leaders Fund and the Ontario Early Researcher Award (Grant Number: #36905). For providing samples, we thank Alan Cain, Steeve Côté, Anh Dao, Marco Festa-Bianchet, Brad Fulk, Eric Hoffman, Levi Jaster, Daniel Koelsch, Emily Latch, Brent Patterson, Joe Nocera, Don Stewart & Russell Easy, Jonathan

Shaw, David Walter and Jon Wheeler. We also thank Jose Alberto López-Alemán for commenting on the text.

We sampled deer from across North America, a stolen land which remains a home to many First Peoples and Trent University is located on the territory of the Michi Saagiig Anishnaabeg. As settlers, we are grateful to have had the opportunity to live and work on this land, and to benefit from it. We would like to show our respect to the First Peoples and thank them for their care, stewardship, and teachings. Miigwetch.

Data Accessibility

Raw reads for the 45 deer additional individuals were deposited on the NCBI Sequence Read Archive (Accession number PRJNA830519). All scripts are available on GitLab (https://gitlab.com/WiDGeT_TrentU/graduate_theses/-/tree/master/Kessler/CH_02).

Author contributions

CK and ABAS conceived the study, ABAS collected the samples, CK performed the molecular laboratory work and the bioinformatic analyses with contribution from ABAS for MSMC2, CK and ABAS wrote the manuscript.

Declaration of interests

CK and ABAS declare no competing interests.

References

Adams KP, Hamilton RJ. 2011. Management History. In: Hewitt DG, editor. Biology and management of white-tailed deer. Boca Raton: CRC Press. Available from: http://site.ebrary.com/id/11007093

Allen JRM, Forrest M, Hickler T, Singarayer JS, Valdes PJ, Huntley B. 2020. Global vegetation patterns of the past 140,000 years. *J Biogeogr* 47:2073–2090.

Allendorf FW, Hard JJ. 2009. Human-induced evolution caused by unnatural selection through harvest of wild animals. *Proc. Natl. Acad. Sci. U.S.A.* 106:9987–9994.

Andrews. 2010. FastQC: a Quality Control Tool for High Throughput Sequence Data. Available online at: http://www.bioinformatics.babraham.ac.uk/projects/fastqc.

Anthony RG, Smith NS. 1977. Ecological Relationships between Mule Deer and White-Tailed Deer in Southeastern Arizona. *Ecological Monographs* 47:255–277.

Baca M. 2020. Diverse responses of common vole (Microtus arvalis) populations to Late Glacial and Early Holocene climate changes - Evidence from ancient DNA. *Quaternary Science Reviews*:13.

Baccus R, Ryman N, Smith MH, Reuterwall C, Cameron D. 1983. Genetic Variability and Differentiation of Large Grazing Mammals. *Journal of Mammalogy* 64:109–120.

Batchelor CL, Margold M, Krapp M, Murton DK, Dalton AS, Gibbard PL, Stokes CR, Murton JB, Manica A. 2019. The configuration of Northern Hemisphere ice sheets through the Quaternary. *Nat Commun* 10:3713.

Bergman EJ, Doherty PF, White GC, Holland AA. 2015. Density dependence in mule deer: a review of evidence. *Wildlife Biology* 21:18–29.

Bolger AM, Lohse M, Usadel B. 2014. Trimmomatic: a flexible trimmer for Illumina sequence data. *Bioinformatics* 30:2114–2120.

Brain RA, Prosser RS. 2022. Human induced fish declines in North America, how do agricultural pesticides compare to other drivers? *Environ Sci Pollut Res* 29:66010–66040.

Broad Institute, GitHub Repository. 2019. “Picard Toolkit.” Available from: http://broadinstitute.github.io/picard/

Brunjes KJ, Ballard WB, Humphrey MH, Harwell F, Mcintyre NE, Krausman PR, Wallace MC. 2006. Habitat Use by Sympatric Mule and White-Tailed Deer in Texas. *Journal of Wildlife Management* 70:1351–1359.

Budd K, Berkman LK, Anderson M, Koppelman J, Eggert LS. 2018. Genetic Structure and Recovery of White-tailed Deer in Missouri. *Jour. Wild. Mgmt.* 82:1598–1607.

Cambronne A. 2013. Deerland: America’s Hunt for Ecological Balance and the Essence of Wildness. Available from:

http://www.freading.com/ebooks/details/r:download/MDAwMDA5LTEwOTA1NDYz

Campbell TA, VerCauteren KC. 2011. Diseases and Parasites. In: Biology and management of white-tailed deer. Boca Raton: CRC Press. p. 220–240. Available from: http://site.ebrary.com/id/11007093

Carr SM, Hughes GA. 1993. Direction of Introgressive Hybridization between Species of North American Deer (Odocoileus) as Inferred from Mitochondrial-Cytochrome-b Sequences. *Journal of Mammalogy* 74:331–342.

Cars BS, Kessler C, Hoffman EA, Côté SD, Koelsch D, Shafer ABA. 2023. Island demographics and trait associations in white-tailed deer. Genomics Available from: http://biorxiv.org/lookup/doi/10.1101/2023.08.01.551454

Ceballos G, Ehrlich PR, Barnosky AD, García A, Pringle RM, Palmer TM. 2015. Accelerated modern human–induced species losses: Entering the sixth mass extinction. *Sci. Adv.* 1:e1400253.

Chafin TK, Zbinden ZD, Douglas MR, Martin BT, Middaugh CR, Gray MC, Ballard JR, Douglas ME. 2021. Spatial Population Genetics in Heavily Managed Species: Separating Patterns of Historical Translocation from Contemporary Gene Flow in White-tailed Deer. *Evol Appl* 14:1673–1689.

Chang CC, Chow CC, Tellier LC, Vattikuti S, Purcell SM, Lee JJ. 2015. Second-generation PLINK: rising to the challenge of larger and richer datasets. *GigaSci* 4:7.

Charlesworth B. 2009. Effective population size and patterns of molecular evolution and variation. *g e n e ti c s*:11.

Chen L, Qiu Q, Jiang Y, Wang K, Lin Z, Li Z, Bibi F, Yang Y, Wang J, Nie W, et al. 2019. Large-scale ruminant genome sequencing provides insights into their evolution and distinct traits. *Science* 364:eaav6202.

Clark PU, Dyke AS, Shakun JD, Carlson AE, Clark J, Wohlfarth B, Mitrovica JX, Hostetler SW, McCabe AM. 2009. The Last Glacial Maximum. *Science* 325:710–714.

Clements D, Young A. 1997. A viewpoint: Rangeland health and mule deer habitat. *JOURNAL OF RANGE MANAGEMENT*.

Colella JP, Lan T, Talbot SL, Lindqvist C, Cook JA. 2021. Whole-genome Resequencing Reveals Persistence of Forest-Associated Mammals in Late Pleistocene Refugia along North America's North Pacific Coast. *J. Biogeogr.* 48:1153–1169.

Combe FJ, Jaster L, Ricketts A, Haukos D, Hope AG. 2021. Population Genomics of Free-ranging Great Plains White-tailed and Mule deer Reflects a Long History of Inter-specific Hybridization. *Evolutionary Applications* 15:111–132.

Commerford JL, Gittens G, Gainforth S, Wilson JJ, Bird BW. 2022. Differences in forest composition following two periods of settlement by pre-Columbian Native Americans. *Veget Hist Archaeobot* 31:467–480.

Cronin MA. 1991. Mitochondrial and Nuclear Genetic Relationships of Deer (Odocoileus spp.) in Western North America. *Can. J. Zool.* 69:1270–1279.

Danecek P, Auton A, Abecasis G, Albers CA, Banks E, DePristo MA, Handsaker RE, Lunter G, Marth GT, Sherry ST, et al. 2011. The variant call format and VCFtools. *Bioinformatics* 27:2156–2158.

Dawe KL, Boutin S. 2016. Climate change is the primary driver of white-tailed deer (Odocoileus virginianus) range expansion at the northern extent of its range; land use is secondary. *Ecol Evol* 6:6435–6451.

De Jong MJ, Li Z, Qin Y, Quéméré E, Baker K, Wang W, Hoelzel AR. 2020. Demography and adaptation promoting evolutionary transitions in a mammalian genus that diversified during the Pleistocene. *Molecular Ecology* 29:2777–2792.

Dedato MN, Robert C, Taillon J, Shafer ABA, Côté SD. 2022. Demographic history and conservation genomics of caribou (Rangifer tarandus) in Québec. *Evolutionary Applications* 15:2043–2053.

Deer Friendly. Deer Population. *Deer Friendly* [Internet]. Available from: https://www.deerfriendly.com/decline-of-deer-populations

Derr JN. 1991. Genetic Interactions between White-Tailed and Mule Deer in the Southwestern United States. *The Journal of Wildlife Management* 55:228.

DeVivo MT, Edmunds DR, Kauffman MJ, Schumaker BA, Binfet J, Kreeger TJ, Richards BJ, Schätzl HM, Cornish TE. 2017. Endemic chronic wasting disease causes mule deer population decline in Wyoming.Zabel MD, editor. *PLoS ONE* 12:e0186512.

Deyoung RW, Demarais S, Honeycutt RL, Rooney AP, Gonzales RA, Gee KL. 2003. Genetic Consequences of White-tailed Deer (Odocoileus virginianus) Restoration in Mississippi. *Molecular Ecology* 12:3237–3252.

Dormann CF, Elith J, Bacher S, Buchmann C, Carl G, Carré G, Marquéz JRG, Gruber B, Lafourcade B, Leitão PJ, et al. 2013. Collinearity: a review of methods to deal with it and a simulation study evaluating their performance. *Ecography* 36:27–46.

Douzery E, Randi E. 1997. The Mitochondrial Control Region of Cervidae: Evolutionary Patterns and Phylogenetic Content. *Molecular Biology and Evolution* 14:1154–1166.

Dussex N, Alberti F, Heino MT, Olsen R-A, van der Valk T, Ryman N, Laikre L, Ahlgren H, Askeyev IV, Askeyev OV, et al. 2020. Moose Genomes Reveal Past Glacial Demography and the Origin of Modern Lineages. *BMC Genomics* 21:854.

Elias S, Schreve D. 2007. Late Pleistocene Megafaunal Extinctions. In: Encyclopedia of Quaternary Science. Elsevier. p. 3202–3217. Available from: https://linkinghub.elsevier.com/retrieve/pii/B0444527478002660

Ellsworth DL, Honeycutt RL, Silvy NJ, Bickham JW, Klimstra WD. 1994. Historical Biogeography and Contemporary Patterns Of Mitochondrial DNA Variation In White-Tailed Deer From The Southeastern United States. *Evolution* 48:122–136.

Ersmark E, Baryshnikov G, Higham T, Argant A, Castaños P, Döppes D, Gasparik M, Germonpré M, Lidén K, Lipecki G, et al. 2019. Genetic turnovers and northern survival during the last glacial maximum in European brown bears. *Ecol Evol* 9:5891–5905.

Evanno G, Regnaut S, Goudet J. 2005. Detecting the Number of Clusters of Individuals Using the Software Structure: a Simulation Study. *Mol Ecol* 14:2611–2620.

Ewels P, Magnusson M, Lundin S, Käller M. 2016. MultiQC: Summarize Analysis Results for Multiple Tools and Samples in a Single Report. *Bioinformatics* 32:3047–3048.

Ferchaud A-L, Perrier C, April J, Hernandez C, Dionne M, Bernatchez L. 2016. Making sense of the relationships between Ne, Nb and Nc towards defining conservation thresholds in Atlantic salmon (Salmo salar). *Heredity* 117:268–278.

Fick SE, Hijmans RJ. 2017. WorldClim 2: new 1-km spatial resolution climate surfaces for global land areas. *International Journal of Climatology* 37:4302–4315.

Forrester TD, Wittmer HU. 2013. A review of the population dynamics of mule deer and black-tailed deer Odocoileus hemionus in North America: Population dynamics of mule deer and black-tailed deer. *Mammal Review* 43:292–308.

Frankham R. 1995. Effective population size/adult population size ratios in wildlife: a review. *Genet. Res.* 66:95–107.

Frankham R. 2005. Genetics and extinction. *Biological Conservation* 126:131–140.

Fulton AE, Yansa CH. 2021. Onset of the Paleoanthropocene in the Lower Great Lakes Region of North America: An Archaeological and Paleoecological Synthesis. *Annals of the American Association of Geographers* 111:771–783.

Fusco NA, Cosentino BJ, Gibbs JP, Allen ML, Blumenfeld AJ, Boettner GH, Carlen EJ, Collins M, Dennison C, DiGiacopo D, et al. 2023. Population genomic structure of a widespread, urban-dwelling mammal: The eastern grey squirrel (*Sciurus carolinensis*). *Molecular Ecology*:mec.17230.

Gajewski K, Kriesche B, Chaput MA, Kulik R, Schmidt V. 2019. Human–vegetation interactions during the Holocene in North America. *Veget Hist Archaeobot* 28:635–647.

Garrison E, Kronenberg ZN, Dawson ET, Pedersen BS, Prins P. 2022. A spectrum of free software tools for processing the VCF variant call format: vcflib, bio-vcf, cyvcf2, hts-nim and slivar.Schneidman-Duhovny D, editor. *PLoS Comput Biol* 18:e1009123.

Gill RB. 1999. Declining Mule Deer Populations in Colorado: Reasons and Responses (a report to the Colorado Legislature, November 1999). 58: Colorado Division of Wildlife

Gowan EJ, Zhang X, Khosravi S, Rovere A, Stocchi P, Hughes ALC, Gyllencreutz R, Mangerud J, Svendsen J-I, Lohmann G. 2021. A new global ice sheet reconstruction for the past 80 000 years. *Nat Commun* 12:1199.

Greenslade AD. 1998. Inter- and intraspecific phylogeography of North American Odocoileus Deer based on mitochondrial DNA sequences. Available from: https://research.library.mun.ca/1190/

Grinberg S. 2019. findPeaks. *GitHub* [Internet]. Available from: https://github.com/stas-g/findPeaks/blob/master/find_peaks.R

Grossen C, Guillaume F, Keller LF, Croll D. 2020. Purging of highly deleterious mutations through severe bottlenecks in Alpine ibex. *Nat Commun* 11:1001.

Gruell GE. 1986. Post-1900 mule deer irruptions in the Intermountain West: Principal cause and influences. Ogden, UT: U.S. Department of Agriculture, Forest Service, Intermountain Research Station Available from: https://www.fs.usda.gov/treesearch/pubs/37804

Gutenkunst RN, Hernandez RD, Williamson SH, Bustamante CD. 2009. Inferring the Joint Demographic History of Multiple Populations from Multidimensional SNP Frequency Data.McVean G, editor. *PLoS Genet* 5:e1000695.

Hahn MW. 2018. Molecular population genetics. New York : Sunderland, MA: Oxford University Press ; Sinauer Associates

Hanberry BB. 2023. Shifting potential tree species distributions from the Last Glacial Maximum to the Mid-Holocene in North America, with a correlation assessment. *J Quaternary Science* 38:829–839.

Heffelfinger J, Krausman PR eds. 2023. Ecology and management of black-tailed and mule deer of North America. First edition. Boca Raton, FL: CRC Press

Hempel E, Bibi F, Faith JT, Koepfli K-P, Klittich AM, Duchêne DA, Brink JS, Kalthoff DC, Dalén L, Hofreiter M, et al. 2022. Blue Turns to Gray: Paleogenomic Insights into the Evolutionary History and Extinction of the Blue Antelope (Hippotragus leucophaeus).Lu J, editor. *Molecular Biology and Evolution* 39:msac241.

Hewitt DG. 2011. Biology and management of white-tailed deer. Boca Raton: CRC Press Available from: http://site.ebrary.com/id/11007093

Hijmans RJ. 2022. raster: Geographic Data Analysis and Modeling. Available from: https://CRAN.R-project.org/package=raster

IPCC. 2022. Climate change 2022: Impacts, adaptation and vulnerability. :3–33.

Ito T, Hayakawa T, Suzuki–Hashido N, Hamada Y, Kurihara Y, Hanya G, Kaneko A, Natsume T, Aisu S, Honda T, et al. 2021. Phylogeographic History of Japanese Macaques. *J Biogeogr*:jbi.14087.

Jensen WF, Bleich VC, Whittaker DG. 2023. Historical Trends in Black-tailed Deer, Mule Deer, and Their Habitats. In: Heffelfinger J, Krausman PR, Cox A, editors. Ecology and management of black-tailed and mule deer of North America. First edition. Boca Raton, FL: CRC Press.

Kessler C, Wootton E, Shafer ABA. 2023. Speciation without gene-flow in hybridizing deer. *Molecular Ecology* 32:1117–1132.

Klassmann A, Gautier M. 2022. Detecting selection using extended haplotype homozygosity (EHH)-based statistics in unphased or unpolarized data.Rashid MAR, editor. *PLoS ONE* 17:e0262024.

Klicka LB, Najar N, Vázquez-Miranda H, Zink R. 2023. Relationships among North American deer based on mitochondrial DNA and ultraconserved elements, with comments on mito-nuclear discordance. In Review Available from: https://www.researchsquare.com/article/rs-3006994/v1

Kopelman NM, Mayzel J, Jakobsson M, Rosenberg NA, Mayrose I. 2015. Clumpak: a Program for Identifying Clustering Modes and Packaging Population Structure Inferences Across K. *Mol Ecol Resour* 15:1179–1191.

Korneliussen TS, Albrechtsen A, Nielsen R. 2014. ANGSD: Analysis of Next Generation Sequencing Data. *BMC Bioinformatics* 15:356.

Kvalnes T, Saether B-E, Haanes H, Røed KH, Engen S, Solberg EJ. 2016. Harvest-induced phenotypic selection in an island population of moose, Alces alces. *Evolution* 70:1486–1500.

Lamb S, Taylor AM, Hughes TA, McMillan BR, Larsen RT, Khan R, Weisz D, Dudchenko O, Aiden EL, Edelman NB, et al. 2021. De novo chromosome-length assembly of the mule deer (Odocoileus hemionus) genome. *Gigabyte* 2021:1–13.

Lapierre M, Lambert A, Achaz G. 2017. Accuracy of Demographic Inferences from the Site Frequency Spectrum: The Case of the Yoruba Population. *Genetics* 206:439–449.

Latch EK, Heffelfinger JR, Fike JA, RHODES Jr OE. 2009. Species-wide Phylogeography of North American Mule Deer (Odocoileus hemionus): Cryptic Glacial Refugia and Postglacial Recolonization. *Molecular Ecology* 18:1730–1745.

Latch EK, Reding DM, Heffelfinger JR, Alcalá-Galván CH, Rhodes OE. 2014. Range-wide Analysis of Genetic Structure in a Widespread, Highly Mobile Species (Odocoileus hemionus) Reveals the Importance of Historical Biogeography. *Mol Ecol* 23:3171–3190.

Legendre P, Legendre L. 2012. Numerical ecology. Elsevier

Li H, Durbin R. 2009. Fast and Accurate Short Read Alignment with Burrows-Wheeler Transform. *Bioinformatics* 25:1754–1760.

Li H, Durbin R. 2011. Inference of human population history from individual whole-genome sequences. *Nature* 475:493–496.

Li H, Handsaker B, Wysoker A, Fennell T, Ruan J, Homer N, Marth G, Abecasis G, Durbin R, 1000 Genome Project Data Processing Subgroup. 2009. The Sequence Alignment/Map format and SAMtools. *Bioinformatics* 25:2078–2079.

Lindo J, Huerta-Sánchez E, Nakagome S, Rasmussen M, Petzelt B, Mitchell J, Cybulski JS, Willerslev E, DeGiorgio M, Malhi RS. 2016. A time transect of exomes from a Native American population before and after European contact. *Nat Commun* 7:13175.

Liu X, Fu Y-X. 2015. Exploring population size changes using SNP frequency spectra. *Nat Genet* 47:555–559.

Liu X, Fu Y-X. 2020. Stairway Plot 2: demographic history inference with folded SNP frequency spectra. *Genome Biol* 21:280.

Loog L, Thalmann O, Sinding MS, Schuenemann VJ, Perri A, Germonpré M, Bocherens H, Witt KE, Samaniego Castruita JA, Velasco MS, et al. 2020. Ancient DNA suggests modern wolves trace their origin to a Late Pleistocene expansion from Beringia. *Mol Ecol* 29:1596–1610.

Lorenzen ED, Nogués-Bravo D, Orlando L, Weinstock J, Binladen J, Marske KA, Ugan A, Borregaard MK, Gilbert MTP, Nielsen R, et al. 2011. Species-specific responses of Late Quaternary megafauna to climate and humans. *Nature* 479:359–364.

Lynch VJ, Bedoya-Reina OC, Ratan A, Sulak M, Drautz-Moses DI, Perry GH, Miller W, Schuster SC. 2015. Elephantid Genomes Reveal the Molecular Bases of Woolly Mammoth Adaptations to the Arctic. *Cell Reports* 12:217–228.

Malhi Y, Doughty CE, Galetti M, Smith FA, Svenning J-C, Terborgh JW. 2016. Megafauna and ecosystem function from the Pleistocene to the Anthropocene. *Proc. Natl. Acad. Sci. U.S.A.* 113:838–846.

Malhi Y, Lander T, Le Roux E, Stevens N, Macias-Fauria M, Wedding L, Girardin C, Kristensen JÅ, Sandom CJ, Evans TD, et al. 2022. The role of large wild animals in climate change mitigation and adaptation. *Current Biology* 32:R181–R196.

Manel S, Perrier C, Pratlong M, Abi-Rached L, Paganini J, Pontarotti P, Aurelle D. 2016. Genomic resources and their influence on the detection of the signal of positive selection in genome scans. *Molecular Ecology* 25:170–184.

Martchenko D, Shafer ABA. 2023. Contrasting whole-genome and reduced representation sequencing for population demographic and adaptive inference: an alpine mammal case study. *Heredity* [Internet]. Available from: https://www.nature.com/articles/s41437-023-00643-4

Martin M, Patterson M, Garg S, O Fischer S, Pisanti N, Klau GW, Schöenhuth A, Marschall T. 2016. WhatsHap: Fast and Accurate Read-based Phasing. Bioinformatics Available from: http://biorxiv.org/lookup/doi/10.1101/085050

Martin S. 2021. genomics_general. *GitHub* [Internet]. Available from: https://github.com/simonhmartin/genomics_general

Mautz W, Pekins P, Warren J. 1985. Cold temperature effects on metabolic rate of white-tailed, mule, and black-tailed deer in winter coat. *Biology of deer production. Bulletin* 22:453–457.

McDonald JS, Miller KV, Association QDM, Resources DBWS of F. 2004. A History of White-tailed Deer Restocking in the United States, 1878 to 2004. Quality Deer Management Assoc. Available from: https://books.google.ca/books?id=fv_oGwAACAAJ

McKenna A, Hanna M, Banks E, Sivachenko A, Cibulskis K, Kernytsky A, Garimella K, Altshuler D, Gabriel S, Daly M, et al. 2010. The Genome Analysis Toolkit: A MapReduce framework for analyzing next-generation DNA sequencing data. *Genome Research* 20:1297–1303.

Meiri M, Lister A, Kosintsev P, Zazula G, Barnes I. 2020. Population dynamics and range shifts of moose (Alces alces) during the Late Quaternary. *J Biogeogr* 47:2223–2234.

Meisner J, Albrechtsen A. 2018. Inferring Population Structure and Admixture Proportions in Low-Depth NGS Data. *Genetics* 210:719–731.

Meltzer DJ. 2020. Overkill, glacial history, and the extinction of North America's Ice Age megafauna. *Proc. Natl. Acad. Sci. U.S.A.* 117:28555–28563.

Moscarella RA, Aguilera M, Escalante AA. 2003. Phylogeography, Population Structure, and Implications for Conservation of White-tailed Deer (Odocoileus Virginianus) in Venezuela. *Journal of Mammalogy* 84:1300–1315.

Mottl O, Flantua SGA, Bhatta KP, Felde VA, Giesecke T, Goring S, Grimm EC, Haberle S, Hooghiemstra H, Ivory S, et al. 2021. Global acceleration in rates of vegetation change over the past 18,000 years. *Science* 372:860–864.

O'Connell J, Gurdasani D, Delaneau O, Pirastu N, Ulivi S, Cocca M, Traglia M, Huang J, Huffman JE, Rudan I, et al. 2014. A General Approach for Haplotype Phasing across the Full Spectrum of Relatedness.Gibson G, editor. *PLoS Genet* 10:e1004234.

Oksanen J, Simpson GL, Blanchet FG, Kindt R, Legendre P, Minchin PR, O'Hara RB, Solymos P, Stevens MHH, Szoecs E, et al. 2022. vegan: Community Ecology Package. Available from: https://CRAN.R-project.org/package=vegan

Palkopoulou E, Mallick S, Skoglund P, Enk J, Rohland N, Li H, Omrak A, Vartanyan S, Poinar H, Götherström A, et al. 2015. Complete Genomes Reveal Signatures of Demographic and Genetic Declines in the Woolly Mammoth. *Current Biology* 25:1395–1400.

Palstra FP, Ruzzante DE. 2008. Genetic estimates of contemporary effective population size: what can they tell us about the importance of genetic stochasticity for wild population persistence? *Molecular Ecology* 17:3428–3447.

Pamilo P, Savolainen O. 2004. Post-Glacial Colonization, Drift, Local Selection and Conservation Value of Populations: A Northern Perspective. *Hereditas* 130:229–238.

Paradis E, Schliep K. 2019. ape 5.0: an environment for modern phylogenetics and evolutionary analyses in R. *Bioinformatics* 35:526–528.

Patterson M, Marschall T, Pisanti N, Van Iersel L, Stougie L, Klau GW, Schönhuth A. 2015. WhatsHap : Weighted Haplotype Assembly for Future-Generation Sequencing Reads. *Journal of Computational Biology* 22:498–509.

Peart CR, Tusso S, Pophaly SD, Botero-Castro F, Wu C-C, Aurioles-Gamboa D, Baird AB, Bickham JW, Forcada J, Galimberti F, et al. 2020. Determinants of genetic variation across eco-evolutionary scales in pinnipeds. *Nat Ecol Evol* 4:1095–1104.

Pedersen BS, Quinlan AR. 2018. Mosdepth: Quick Coverage Calculation for Genomes and Exomes.Hancock J, editor. *Bioinformatics* 34:867–868.

Peres TM, Altman H. 2018. The Magic of Improbable Appendages: Deer Antler Objects in the Archaeological Record of the American South. *Journal of Archaeological Science: Reports* 20:888–895.

Portik DM, Leaché AD, Rivera D, Barej MF, Burger M, Hirschfeld M, Rödel M, Blackburn DC, Fujita MK. 2017. Evaluating mechanisms of diversification in a Guineo-Congolian tropical forest frog using demographic model selection. *Mol Ecol* 26:5245–5263.

Pundir S, Martin MJ, O'Donovan C, The UniProt Consortium. 2016. UniProt Tools. *Current Protocols in Bioinformatics* [Internet] 53. Available from: https://onlinelibrary.wiley.com/doi/10.1002/0471250953.bi0129s53

R Core Team. 2021. R: A Language and Environment for Statistical Computing. Vienna, Austria: R Foundation for Statistical Computing Available from: https://www.R-project.org/

Robin M, Ferrari G, Akgül G, Münger X, Von Seth J, Schuenemann VJ, Dalén L, Grossen C. 2022. Ancient mitochondrial and modern whole genomes unravel massive genetic diversity loss during near extinction of Alpine ibex. *Molecular Ecology* 31:3548–3565.

Roycroft E, MacDonald AJ, Moritz C, Moussalli A, Portela Miguez R, Rowe KC. 2021. Museum genomics reveals the rapid decline and extinction of Australian rodents since European settlement. *Proc Natl Acad Sci USA* 118:e2021390118.

Russell T, Cullingham C, Ball M, Pybus M, Coltman D. 2021. Extent and direction of introgressive hybridization of mule and white-tailed deer in western Canada. *Evol Appl* 14:1914–1925.

Sabeti PC, Reich DE, Higgins JM, Levine HZP, Richter DJ, Schaffner SF, Gabriel SB, Platko JV, Patterson NJ, McDonald GJ, et al. 2002. Detecting recent positive selection in the human genome from haplotype structure. *Nature* 419:832–837.

Santiago E, Novo I, Pardiñas AF, Saura M, Wang J, Caballero A. 2020. Recent Demographic History Inferred by High-Resolution Analysis of Linkage Disequilibrium.Kim Y, editor. *Molecular Biology and Evolution* 37:3642–3653.

Schiffels S, Durbin R. 2014. Inferring Human Population Size and Separation History from Multiple Genome Sequences. *Nat Genet* 46:919–925.

Schiffels S, Wang K. 2020. MSMC and MSMC2: The Multiple Sequentially Markovian Coalescent. In: Dutheil JY, editor. Statistical Population Genomics. Vol. 2090. Methods in Molecular Biology. New York, NY: Springer US. p. 147–166. Available from: https://link.springer.com/10.1007/978-1-0716-0199-0_7

Seabury CM, Oldeschulte DL, Bhattarai EK, Legare D, Ferro PJ, Metz RP, Johnson CD, Lockwood MA, Nichols TA. 2020. Accurate Genomic Predictions for Chronic Wasting Disease in U.S. White-Tailed Deer. *G3 Genes|Genomes|Genetics* 10:1433–1441.

Shafer ABA, Cullingham CI, Côté SD, Coltman DW. 2010. Of Glaciers and Refugia: a Decade of Study Sheds New Light on the Phylogeography of Northwestern North America. *Molecular Ecology* 19:4589–4621.

Shafer ABA, Gattepaille LM, Stewart REA, Wolf JBW. 2015. Demographic inferences using short-read genomic data in an approximate Bayesian computation framework: in silico evaluation of power, biases and proof of concept in Atlantic walrus. *Mol Ecol* 24:328–345.

Skotte L, Korneliussen TS, Albrechtsen A. 2013. Estimating Individual Admixture Proportions from Next Generation Sequencing Data. *Genetics* 195:693–702.

Smith BT, Gehara M, Harvey MG. 2021. The demography of extinction in eastern North American birds. *Proc. R. Soc. B.* 288:20201945.

Soltis DE, Morris AB, McLACHLAN JS, Manos PS, Soltis PS. 2006. Comparative phylogeography of unglaciated eastern North America. *Molecular Ecology* 15:4261–4293.

Stevens N, Bond W, Feurdean A, Lehmann CER. 2022. Grassy Ecosystems in the Anthropocene. *Annu. Rev. Environ. Resour.* 47:261–289.

Stewart M, Carleton WC, Groucutt HS. 2021. Climate change, not human population growth, correlates with Late Quaternary megafauna declines in North America. *Nat Commun* 12:965.

Stuart AJ. 2015. Late Quaternary megafaunal extinctions on the continents: a short review: LATE QUATERNARY MEGAFAUNAL EXTINCTIONS. *Geol. J.* 50:338–363.

Szpiech ZA. 2021. selscan 2.0: scanning for sweeps in unphased data. Evolutionary Biology Available from: http://biorxiv.org/lookup/doi/10.1101/2021.10.22.465497

Tarasov A, Vilella AJ, Cuppen E, Nijman IJ, Prins P. 2015. Sambamba: fast processing of NGS alignment formats. *Bioinformatics* 31:2032–2034.

Tavares GM, Reales G, Bortolini MC, Fagundes NJR. 2019. Measuring the impact of European colonization on Native American populations in Southern Brazil and Uruguay: Evidence from mtDNA. *Am J Hum Biol* 31:e23243.

Taylor RS, Manseau M, Klütsch CFC, Polfus JL, Steedman A, Hervieux D, Kelly A, Larter NC, Gamberg M, Schwantje H, et al. 2021. Population dynamics of caribou shaped by glacial cycles before the last glacial maximum. *Mol Ecol*:mec.16166.

U.S. Fish & Wildlife Service. 1967. Endangered Species List.

Van De Walle J, Pigeon G, Zedrosser A, Swenson JE, Pelletier F. 2018. Hunting regulation favors slow life histories in a large carnivore. *Nat Commun* 9:1100.

Villanova VL, Hughes PT, Hoffman EA. 2017. Combining genetic structure and demographic analyses to estimate persistence in endangered Key deer (Odocoileus virginianus clavium). *Conserv Genet* 18:1061–1076.

Voight BF, Kudaravalli S, Wen X, Pritchard JK. 2006. A Map of Recent Positive Selection in the Human Genome.Hurst L, editor. *PLoS Biol* 4:e72.

Wang K, Mathieson I, O'Connell J, Schiffels S. 2020. Tracking Human Population Structure through Time from Whole Genome Sequences.Schierup MH, editor. *PLoS Genet* 16:e1008552.

Waples RS, Luikart G, Faulkner JR, Tallmon DA. 2013. Simple life-history traits explain key effective population size ratios across diverse taxa. *Proc. R. Soc. B.* 280:20131339.

Webb GK. 2018. Searching the internet to estimate deer population trends in the U.S., California, and Connecticut. *IIS* 19:163–173.

Weitzel EM. 2021. Investigating overhunting of white-tailed deer (Odocoileus virginianus) in the late Holocene Middle Tennessee River Valley. *Southeastern Archaeology* 40:1–19.

Wilder AP, Supple MA, Subramanian A, Mudide A, Swofford R, Serres-Armero A, Steiner C, Koepfli K-P, Genereux DP, Karlsson EK, et al. 2023. The contribution of historical processes to contemporary extinction risk in placental mammals. *Science* 380:eabn5856.

Willerslev E, Meltzer DJ. 2021. Peopling of the Americas as inferred from ancient genomics. *Nature* 594:356–364.

Woinarski JCZ, Burbidge AA, Harrison PL. 2015. Ongoing unraveling of a continental fauna: Decline and extinction of Australian mammals since European settlement. *Proc. Natl. Acad. Sci. U.S.A.* 112:4531–4540.

Wolverton S, Nagaoka L, Densmore J, Fullerton B. 2008. White-tailed deer harvest pressure & within-bone nutrient exploitation during the mid- to late Holocene in southeast Texas. *Before Farming* 2008:1–23.

Wootton E, Robert C, Taillon J, Côté SD, Shafer ABA. 2023. Genomic health is dependent on long-term population demographic history. *Molecular Ecology* 32:1943–1954.

Wright EA, Roberts EK, Platt RN, Bayouth JV, Conway WC, Bradley RD. 2022. Mitochondrial capture and subsequent genetic divergence generates a novel haplogroup: evidence from ancient and ongoing hybridization in mule and white-tailed deer. *Journal of Mammalogy* 103:723–736.

Zamorano LS, Gompert Z, Fronhofer EA, Feder JL, Nosil P. 2023. A stabilizing eco-evolutionary feedback loop in the wild. *Current Biology* 33:3272-3278.e3.

Tables

Table 1: Tajima's D, nucleotide diversity and F_{ROH} for our four populations, F_{ROH} as percentage of the N90 scaffolds.

	Tajima's D	**Nucleotide diversity (π)**	**F_{ROH}**
WTD_{ML}	-0.76	0.0068	0.89
WTD_{KEY}	0.70	0.0038	1.38
MD_{MD}	0.81	0.0036	0.30
MD_{BTD}	1.08	0.0037	0.28

Table 2: Anova of the RDA for full and conditional models as well as number of outlier SNPs for each predictor in the full model. Significant p-values are highlighted in bold.

		Adjusted R^2	bio1	bio2	bio8	bio12	bio14	bio15	bio16	bio18	Longitude	Species
Interspecies												
~ BIOs + Long + SP	P-value	16.55%	**0.004**	**0.001**	**0.012**	**0.009**	-	**0.001**	-	-	**0.001**	**0.001**
	Variance explained		2.58%	3.12%	1.95%	1.95%	-	3.54%	-	-	3.55%	7.96%
	number of outlier SNPs		5448	768	760	2491		47			2820	2101
MD												
~ BIOs + Long	P-value	8.82%	0.093	**0.001**	-	-	0.116	0.355	**0.012**	0.374	0.219	-
	Variance explained		5.67%	9.82%	-	-	5.48%	4.82%	6.72%	4.83%	5.04%	-
	number of outlier SNPs		99	540	-	-	690	1	4452	0	1652	-
~ BIOs + Condition(Long)	P-value	4.11%	0.119	**0.032**	-	-	0.167	0.336	**0.003**	0.476	-	-
	Variance explained		5.96%	6.23%	-	-	5.84%	5.53%	7.29%	5.35%	-	-
~ Condition(BIOs) + Long	P-value	0.35%	-	-	-	-	-	-	-	-	0.445	-
	Variance explained		-	-	-	-	-	-	-	-	8.05%	-
WTD												
~ BIOs + Long	P-value	6.32%	**0.001**	**0.001**	**0.034**	-	-	**0.001**	-	-	**0.001**	-
	Variance explained		3.37%	3.89%	2.11%	-	-	2.99%	-	-	2.96%	-
	number of outlier SNPs		5625	4487	1025	-	-	209	-	-	777	-
~ BIOs + Condition(Long)	P-value	4.64%	**0.001**	**0.001**	**0.038**	-	-	**0.001**	-	-	-	-
	Variance explained		3.50%	3.57%	2.18%	-	-	2.94%	-	-	-	-
~ Condition(BIOs) + Long	P-value	1.26%	-	-	-	-	-	-	-	-	**0.001**	-
	Variance explained		-	-	-	-	-	-	-	-	3.38%	-

Figures

A

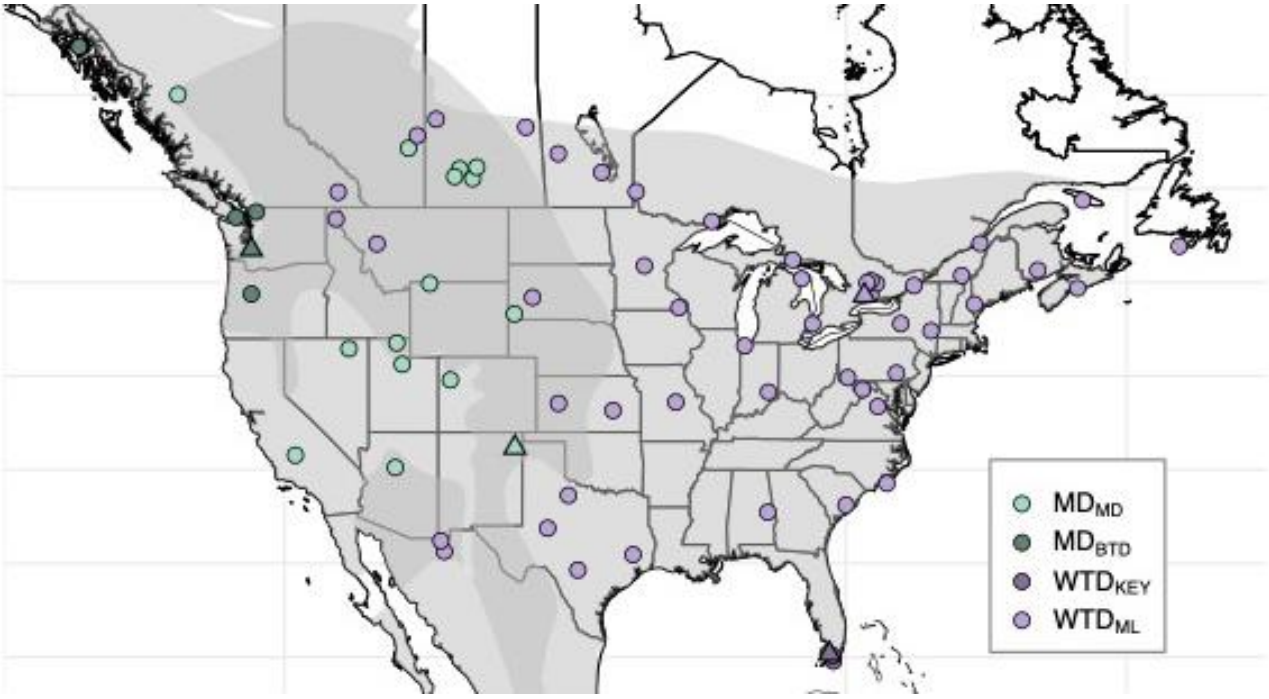

B

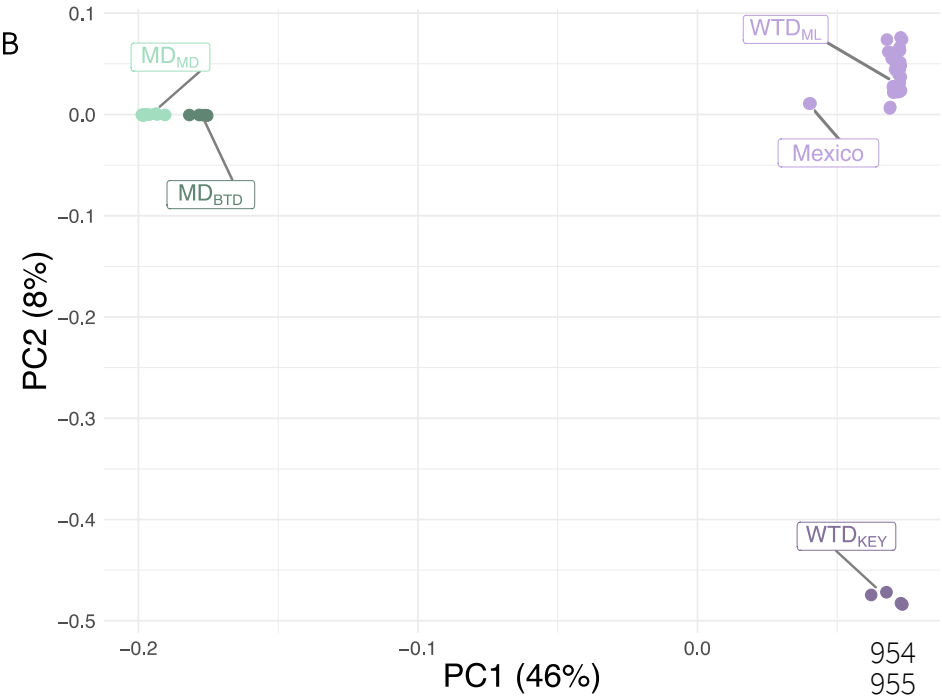

Figure 1: Sample information. (A) Sampling locations and population assignment, triangles represent high-coverage samples, shaded areas represent each species' IUCN range with areas of sympatry in a daker shade (B) PCA of all individuals, based on allele frequencies. Colour coded by assigned population.

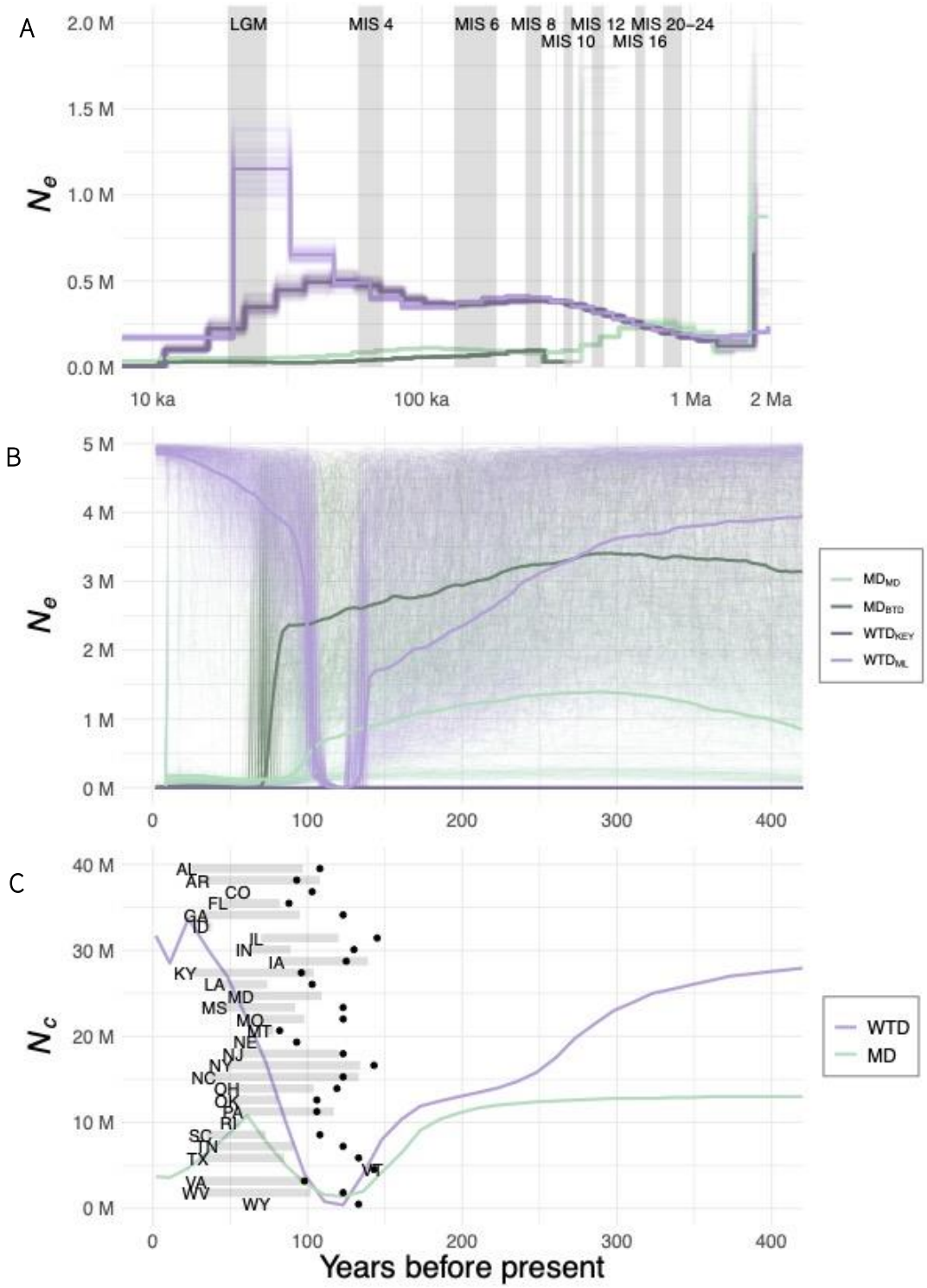

Figure 2: Demographic inference. (A) Changes in population size of four high coverage samples with bootstraps as estimated by MSMC2, shaded areas symbolise full glacial periods (Batchelor et al. 2019). (B) Recent changes in N_e computed by GONE on all samples with bootstraps. (C) Estimated WTD & MD population in the US from Webb (2018) with WTD restocking period for 30 US states (grey rectangles) and corresponding state's year with lowest WTD population (black points) from McDonald et al. (2004).

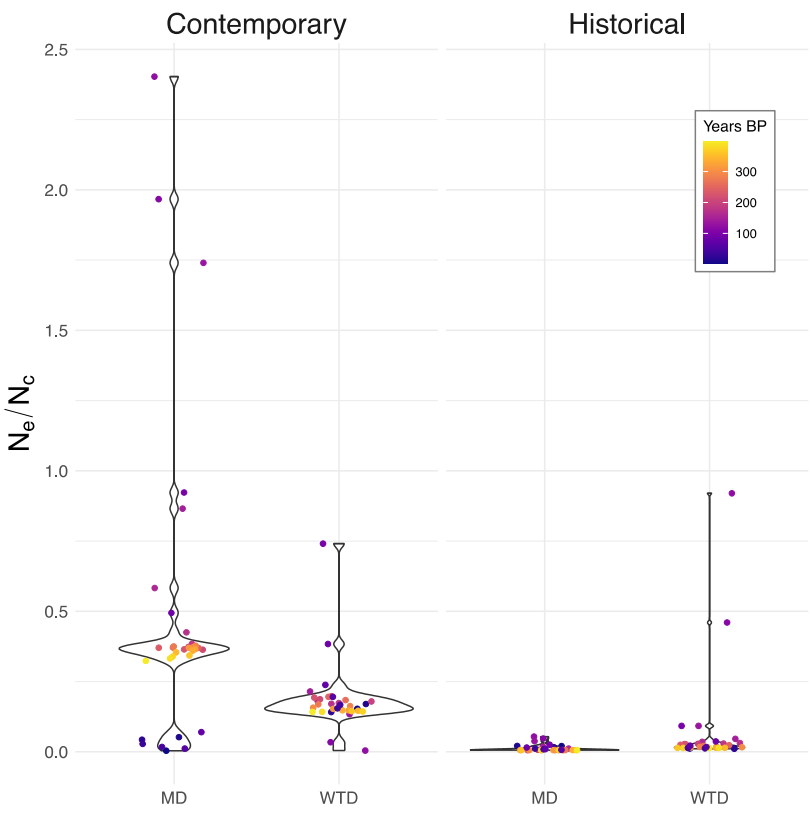

Figure 3: Contemporary and historical N_e/N_c ratio over time, point colour indicates time before present, N_e of the historical ratio taken from NuA values in the δaδi analysis.

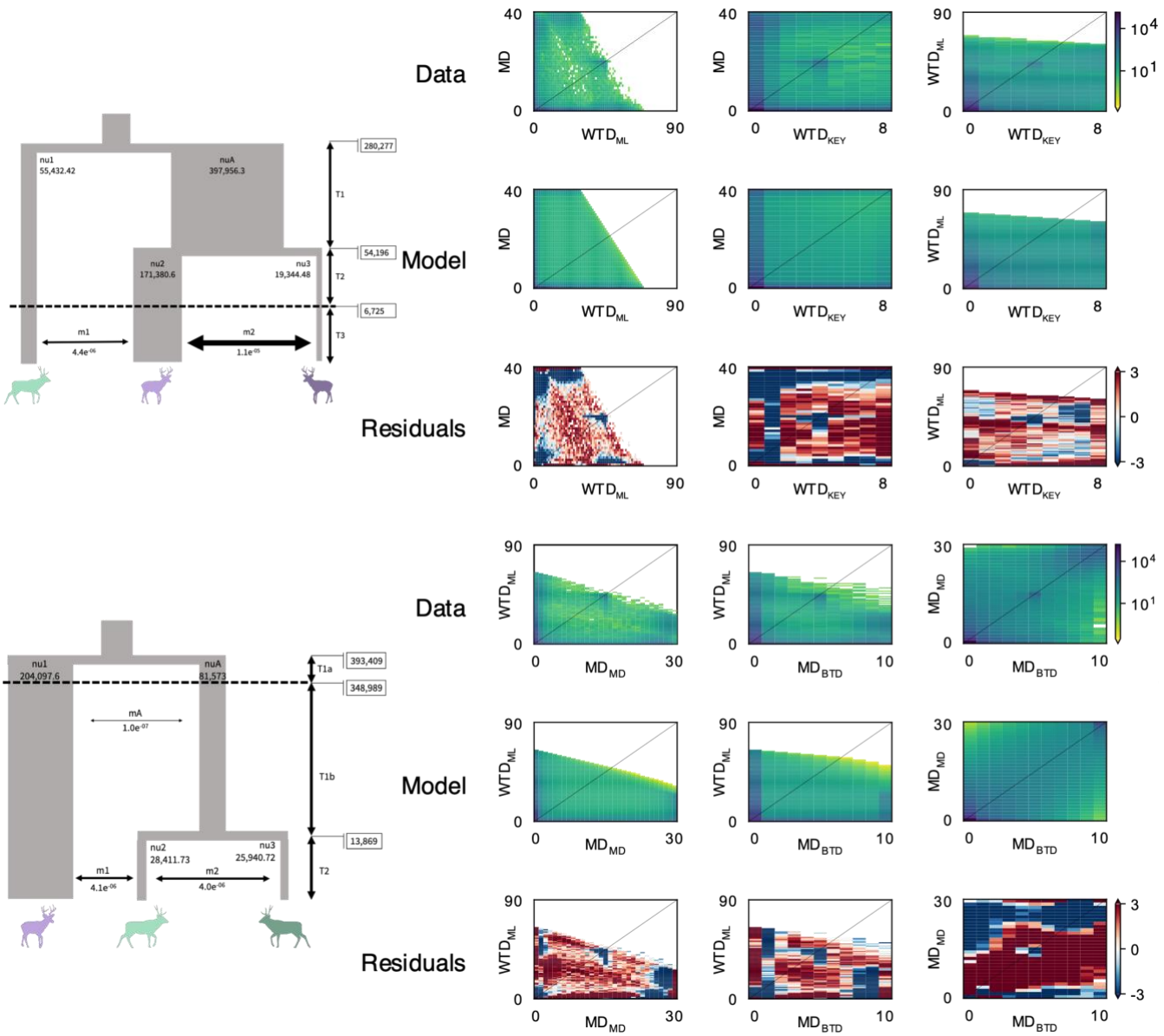

Figure 4: Three populations models in δaδI with best model schema on the left and 2D spectra on the right. (A) MD – WTD_{ML} – WTD_{KEY} comparisons, with MD in green, WTD_{ML} in light and WTD_{KEY} in dark purple. (B) WTD_{ML} – MD_{MD} – MD_{BTD} comparison with WTD_{ML} in light purple, MD_{MD} in light green and MD_{BTD} in dark green. Population sizes (nu) and migration rates (m) estimates to scale, time is not to scale.